20th International Conference
ENGINEERING MECHANICS 2014
Svratka, Czech Republic, 12 – 15 May 2014

PARALLEL NUMERICAL COMPUTATION OF DISTRIBUTION OF PRESURE PAST AN OSCILATING AIRFOIL NACA0015

V. Řidký[*], P. Šidlof[**]

Abstract: *The article is devoted to 2D parallel numerical computation of pressure on the surface of an elastically supported airfoil self-oscillating due to interaction with the airflow. Movement of airfoil is described by translation and rotation, identified from experimental data. A new boundary condition for the 2DOF motion of the airfoil was implemented in OpenFoam, an open-source software package based on finite volume method. The results of numerical simulation (distribution of pressure on the surface of airfoil) are compared with experimental data measured in a wind tunnel, where a physical model of NACA0015 airfoil was mounted and tuned to exhibit the flutter instability. The experimental results were obtained previously in the Institute of Thermomechanics by interferographic measurement in a subsonic wind tunnel.*

Keywords: OpenFOAM, Airfoil, Parallel computing and dynamic mesh.

1. Introduction

Numerical simulation of flow around an oscillating NACA0015 airfoil is a very complex problem. In this case is coupled a problematic of numerical solution of a flow and the interaction of fluids and elastic structures. The airfoil can be approximated as a two-degree-of-freedom system, with vertical translation and rotation modes. Movement is harmonic with constant amplitude (flutter instability). This movement is described below.

The numerical solution of interaction of fluids and elastic structures are very often time consuming. Flow around an oscillating airfoil is complex and during large angles of -attack massive flow separation may occur. In aerospace engineering applications, flow is almost always turbulent. Two-dimensional models are still applied from practical reasons, mainly because the computational cost is drastically lower. For the numerical simulation of laminar and turbulent flow is possible to use the following approaches. The most frequent in CFD are RANS model (Reynolds Averaged Navier-Stokes equations). Because the Navier Stokes equations are nonlinear after averaging arises a new term the Reynolds stress. This term is modelled. In this case a two equations model k-ω SST (Menter, 1994) is used. This model gives good results in adverse pressure gradients and separating flows. Next possibility how model the turbulent flow is used LES (Large Eddy Simulations). The solutions of the Navier-Stokes equations are divided into two parts. Large coherent turbulent structures are solved directly and the small-scale isotropic turbulence is modelled. The third possibility is the Direct Numerical Simulations (DNS), which solve directly the Navier-Stokes equations. Element size corresponds to the smallest scales of turbulence, this is the reason why the mesh must be fine enough. The number of elements scales with $Re^{9/4}$.

This paper is focused on 2D numerical solution of incompressible and compressible airflow past the airfoil. The distribution of p/p0 on the surface of the airfoil when using incompressible model of flow (without turbulence model and SST k-ω model turbulence) and compressible model of flow (without turbulence model) is compared. The results of numerical simulations are compared with experimental data measured in aerodynamic tunnel of the Institute of Thermomechanics in Nový Knín. In the experiment, the pressures are evaluated from interferograms obtained using Mach-Zehnder interferometer, as described in (Vlček, 2010).

[*] Ing. Václav Řidky: Technical University of Liberec, Studentská 2, Liberec 461 17; CZ, vaclav.ridky@tul.cz
[**] Ing. Petr Šidlof, PhD.: Technical University of Liberec, Studentská 2, Liberec 461 17; CZ, sidlof@it.cas.cz

2. Methods

Numerical simulation is solved in software package OpenFoam (finite volume method) and the meshes are created in mesh generator GridPro. For the mathematical description of flow around the airfoil are used incompressible (1), (2) and compressible (3), (4) Navier-Stokes equations.

$$\nabla \cdot \boldsymbol{u} = 0 \tag{1}$$

$$\frac{\partial \boldsymbol{u}}{\partial t} + \nabla \cdot (\boldsymbol{uu}) - \nabla \cdot \nu \nabla \boldsymbol{u} + \frac{1}{\rho}\nabla p = 0 \tag{2}$$

$$\frac{\partial \rho}{\partial t} + \nabla \cdot (\rho \boldsymbol{u}) = 0 \tag{3}$$

$$\frac{\partial \rho \boldsymbol{u}}{\partial t} + \nabla \cdot (\rho \boldsymbol{uu}) - \nabla \cdot \mu \nabla \boldsymbol{u} + \nabla p = 0 \tag{4}$$

Here u, p and ρ are fluid velocity, pressure, and density, ν is kinematic viscosity and μ is dynamic viscosity. For the compressible flow is needed also equation for heat transfer. When the k-ω SST turbulence model is used, the equation for k (turbulence kinetic energy) and ω (specific dissipation rate) is necessary:

$$\frac{\partial k}{\partial t} + U_j \frac{\partial k}{\partial x_j} = P_k - \beta^* k\omega + \frac{\partial}{\partial x_j}\left[(\nu + \sigma_k \nu_T)\frac{\partial k}{\partial x_j}\right] \tag{5}$$

$$\frac{\partial \omega}{\partial t} + U_j \frac{\partial \omega}{\partial x_j} = \propto S^2 - \beta^* \omega^2 + \frac{\partial}{\partial x_j}\left[(\nu + \sigma_k \nu_T)\frac{\partial \omega}{\partial x_j}\right] + 2(1 - F_1)\sigma_{\omega 2}\frac{1}{\omega}\frac{\partial k}{\partial x_i}\frac{\partial \omega}{\partial x_j} \tag{6}$$

$$\mu_t = \frac{\rho a_1 k}{max(a_1\omega, \Omega F_2)}; F_2 = tanh\left(\left(max\left[\frac{2\sqrt{k}}{\beta^*\omega y}, \frac{500\nu}{y^2\omega}\right]\right)^2\right); P_k = \min\left(\tau_{ij}\frac{\partial U_i}{\partial x_j} k\omega 10\beta^*\right) \tag{7}$$

$$F_1 = \tanh\left\{\left(min\left(max\left[\frac{\sqrt{k}}{\omega y \beta^*}, \frac{500\nu}{y^2\omega}\right], \frac{4\sigma_{\omega 2} k}{CD_{k\omega} y^2}\right)\right)^4\right\};\ CD_{k\omega} = max\left(2\rho\sigma_{\omega 2}\frac{1}{\omega}\frac{\partial k}{\partial x_i}\frac{\partial \omega}{\partial x_i}, 10^{-10}\right) \tag{8}$$

$$\alpha_1 = \frac{5}{9}, \alpha_2 = 0.44, \beta_1 = \frac{3}{40}, \beta_1 = 0.0828, \beta^* = \frac{9}{100}, \sigma_{k1} = 0.85, \sigma_{k2} = 1, \sigma_{\omega 1} = 0.5, \sigma_{\omega 2} = 0.856$$

The 2D Geometry corresponds to the experimental setup. OpenFoam. Mesh used for numerical simulation is a c-type mesh and number of element is 80000. Boundary condition for velocity, pressure and movement are same for all cases. Movement of the airfoil is prescribed as boundary condition on boundary (Γ_{wing}). This boundary was implement to OpenFoam and the movement with two degrees of freedom has several parameters. Parameters are frequency 19.5 Hz, the amplitude of the plunging movement was ± 7 mm, the amplitude of the rotational movement is ± 17 ° and phase shift between translation and rotation is 8 ° (Vlček, 2011).

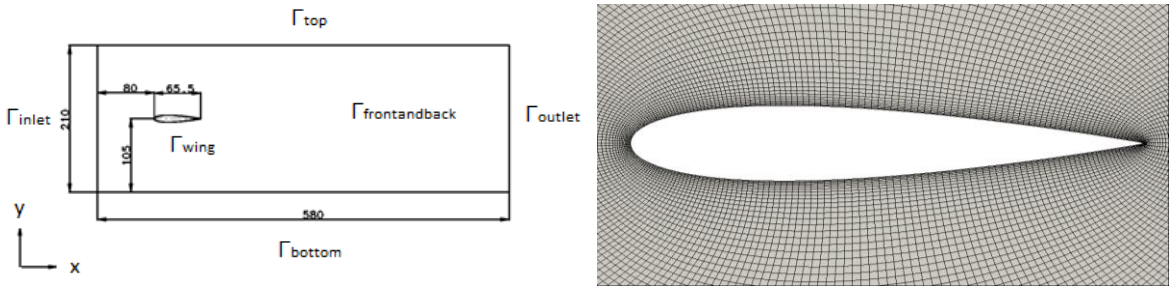

Fig. 1: Computational domain with boundary condition (left) and c-mesh around the airfoil (right).

Following boundary conditions for velocity were prescribed: on input (Γ_{inlet}) is prescribed velocity u = 147 m/s. On the walls of channel (Γ_{top} and Γ_{bottom}) is prescribed velocity u = 0 m/s. On the surface of the wing (Γ_{wing}) is prescribed velocity which corresponds to local velocity of the airfoil movement. Due to large intensity of vorticity resulting from flow separation downstream of the wing surface a stabilized boundary condition is prescribed at outlet Γ_{out}: condition $\partial u / \partial n = 0$ when velocity direction points outward of the domain, u = 0 m/s otherwise. Boundary conditions for the pressure at the inlet (Γ_{out}) prescribe p = 98925 Pa. All walls (Γ_{outlet}, Γ_{top}, *and* Γ_{bottom}) have the Neumann boundary condition $\partial p / \partial n = 0$.

For compressible flow without turbulence model is added boundary condition for temperature. On all surfaces is prescribed temperature measured during the experiment (293 °K). For turbulent variable is on the input (Γ_{inlet}) and output (Γ_{out}) value for k = 85 m^2/s^2 and for ω = 940 1/s. On the other wall (Γ_{wing}, Γ_{top} *and* Γ_{bottom}) are wall functions because thickness first element on the surface of the airfoil is $y^+ = 20$.

3. Results

Results from numerical simulations (pressure) is normalized using reference pressure, because experimental data are also normalized. Value of the pressure is averaged over five periods of vibration. On the graphs (Figs. 2-6) are results in the phases. The zero pitch of the airfoil occurs near phase 013, the time interval between the phases is 2 ms and between phase 006 and phase 010 is 4 ms (index of phase is number of milliseconds from the top position of rotation). The graphs show the normalized pressure field around the airfoil in four specific phases of one vibration period T = 51.3 ms. On the graphs are compared normalized pressure distribution p/p_0 on the surface of the airfoil on the left side are results from top surface of the airfoil and on the right side are results from bottom surface of the airfoil.

All models indicate the same position of the stagnation point and are conforming to the experiment. In the current numerical simulations, the best agreement with the experimental data is obtained using the incompressible simulation with the k-ω SST turbulence model.

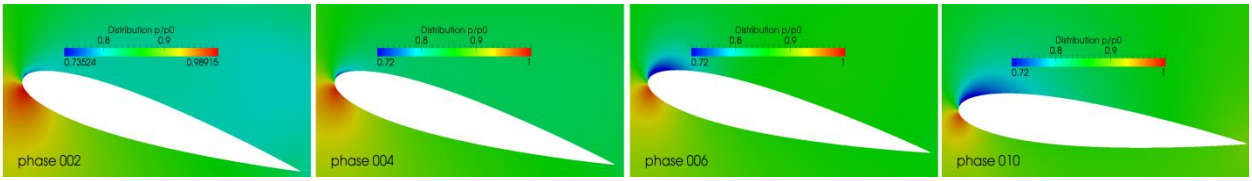

Fig. 2: Normalized pressure distribution p/p_0 for incompressible flow with turbulence model on the surface of the airfoil from numerical simulation and demonstration phase of rotation.

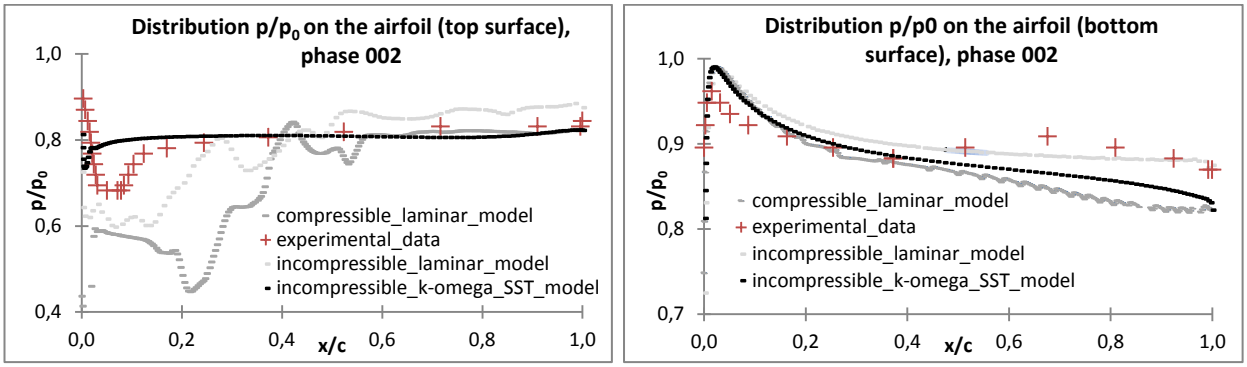

Fig. 3: Normalized pressure distribution p/p_0 on the surface of the airfoil from experiment and numerical simulation, on the left is result on the top surface, on the rights is result on the bottom surface, phase 002.

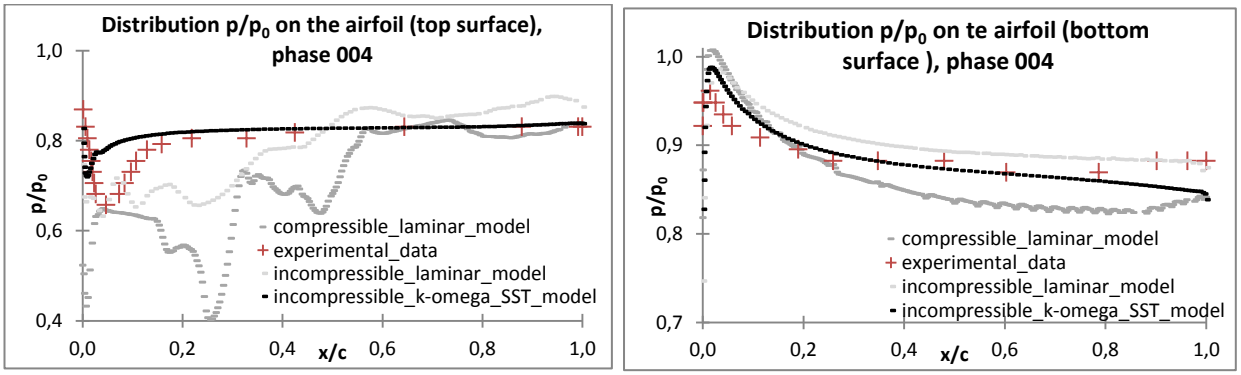

Fig. 4: Normalized pressure distribution p/p_0 on the surface of the airfoil from experiment and numerical simulation, on the left is result on the top surface, on the rights is result on the bottom surface, phase 004.

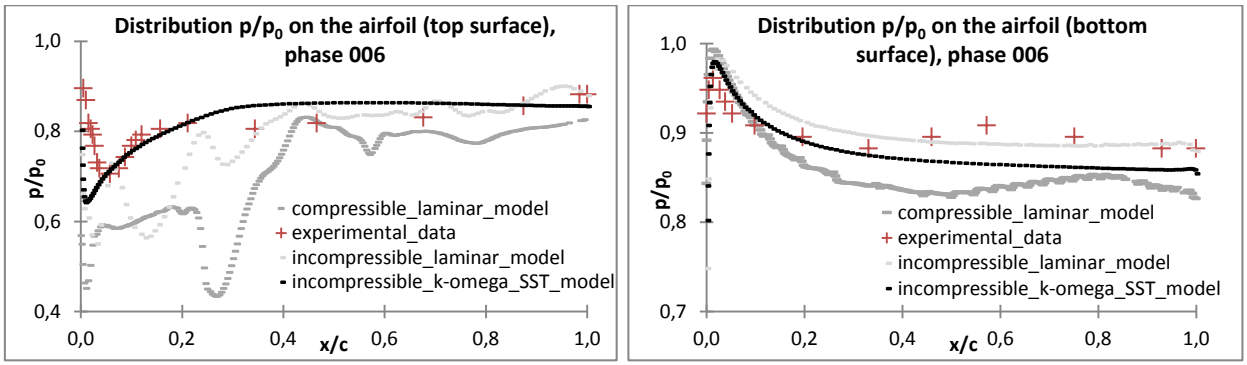

Fig. 5: Normalized pressure distribution p/p_0 on the surface of the airfoil from experiment and numerical simulation, on the left is result on the top surface, on the rights is result on the bottom surface, phase 006.

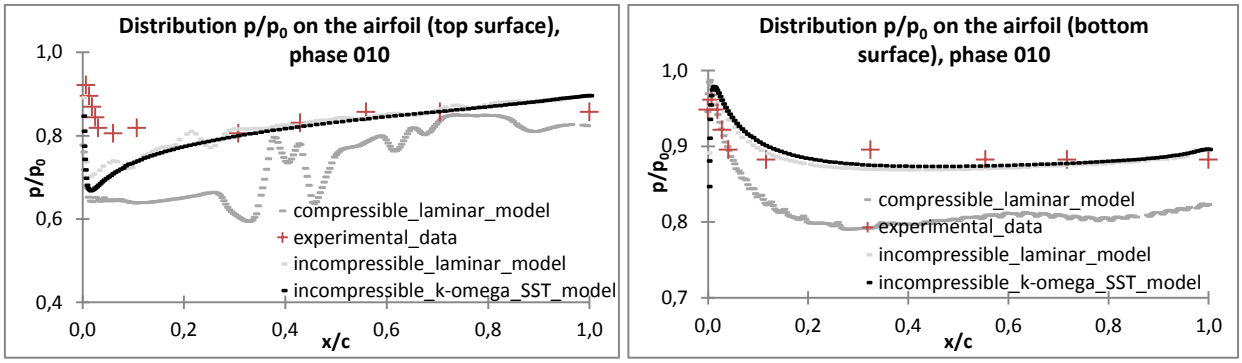

Fig. 6: Normalized pressure distribution p/p_0 on the surface of the airfoil from experiment and numerical simulation, on the left is result on the top surface on the rights is result on the bottom surface, phase 010.

4. Conclusions

Numerical simulations of airflow past a vibrating airfoil were performed and compared with experimental data. Model without model of turbulence provides good match with the experimental data only in the regions, where there is no flow separation. In the separated regions, the results of numerical simulations without turbulence model and experiments are very different. The evaluation of the interferographic images, on the other hand, is also problematic, especially in the regions of high density gradients. But SST k-ω model turbulence gives satisfactory results in the separated region. Problem is here placed where the flow separates. In numerical solution the flow separation point is close to the leading edge. In the experiment the flow separates at approximately 0.07 of the chord length. The difference may be caused by the surface roughness of the physical model.

Acknowledgement

The research has been supported by the Czech Science Foundation, project 13-10527S "Subsonic flutter analysis of elastically supported airfoils using interferometry and CFD". We also wish to acknowledge the help of Dr. Václav Vlček, who provided the data from previous measurements in the wind tunnel.

References

Menter, F. R. (1994) Two-Equation Eddy-Viscosity Turbulence Models for Engineering Applications, AIAA Journal, 32, 8. pp. 1598-1605.

Vlček, V., Kozánek, J., Zolotarev, I. (2011) Forces acting on the fluttering profile in the wind tunnel. Vibration problems ICOVP 2011 - Supplement, 10, pp. 516-522.

Vlček, V., Kozánek, J. (2010) Preliminary interferometry measurements of flow field around a fluttering NACA0015 profile. Engineering Mechanics 2010, 12, pp. 540-550.